

IMPROVING FRT CAPABILITY OF DFIG WITH SMES-FCL UNDER DIFFERENT FAULT CONDITIONS

Vijay A
Department of Electrical and
Electronics Engineering
Government College of
Technology
Coimbatore
er.vijay45@gmail.com

Dr.E.Latha Mercy
Associate Professor
Department of Electrical
and Electronics Engineering
Government College of
Technology
Coimbatore
mercy@gct.ac.in

Mohamed Abdul Kalam M
Department of Electrical
and Electronics Engineering
Government College of
Technology
Coimbatore
eeeabdul54@gmail.com

Ronald S.Ebenezer,
Department of Electrical and
Electronics Engineering
PSG Tech
Coimbatore
Ronaldsebenezer7@gmail.com

Abstract—

In grid-connected Doubly Fed Induction Generators (DFIGs), Fault Ride-Through (FRT) capability and transient stability are vital problems that need to be addressed. In the proposed system a novel Superconducting Magnetic Energy Storage-Fault Current Limiter (SMES-FCL) based protection scheme by modified control of Superconducting Coil (SC) and Rotor Side Converter (RSC) is analysed. The rotor-side mathematical model is used for optimising the value of SC inductance. Two control strategies of SMES-FCL cooperative operation and Positive-sequence $d-q$ Current Modification (PCM) are proposed to control the Grid Side Converter (GSC) and RSC for improving transient stability of the overall performance of the DFIG system. Simulation results obtained from a 1.5 MW DFIG-based wind turbine shows that the proposed system is capable of limiting the peak values of fault rotor current, DC-link voltage and electromagnetic torque under symmetrical and asymmetrical faults, and thus protect the RSC, gearbox and mechanical parts of the whole DFIG. In addition to that, the PCM control scheme is used to lower the Superconducting Coil (SC) current capacity and to smooth the active power of the DFIG during normal operations.

Keywords— Doubly Fed Induction Generator (DFIG), Fault Ride Through (FRT), Superconducting Magnetic Energy Storage Fault Current Limiter (SMES-FCL).

I. INTRODUCTION

Doubly Fed Induction Generator (DFIG) has become the most important choice for wind farms all over the world because of the advantages such as good control ability, high energy efficiency and low capital cost, [1, 2]. Comparing with the other generator, Fault Ride-Through (FRT) capability of DFIG is more vulnerable to grid fault or disturbance [3] because its stator is directly connected to grid, while its rotor is connected to grid by Rotor-Side Converter (RSC) and Grid-Side Converter (GSC) [4]. The RSC and GSC are connected back-to-back through a DC-link capacitor. During grid fault, the stator flux will contain negative-sequence and DC components that induce a large

Electro Motive Force (EMF) in the rotor circuit. Thus, a high rotor over-current and over voltage will be generated in the rotor side converter (RSC) and DC link capacitor side, respectively [5]. These will cause heavy damage of the whole converter. In practice, grid-connected wind turbines (WTs) must ride through grid fault to prevent the damage to the core electrical and mechanical parts of the DFIGs.

From the literature survey, the existing methods to improve the FRT capability can be classified into two categories: control improvement and hardware modification. Some methods are used to reduce the over current during grid fault, or improve the transient stability of WT by modifying GSC or RSC control such as demagnetising current control and dual control techniques [6, 7]. Even though the Control improvement methods might be less costly, the behaviour of DFIG not good during some deep voltage sags because of the confined capacity of RSC [8].

There are various hardware modifications have been proposed to rectify those deep sags. Conventional crowbar and chopper scheme is widely used to reduce the rotor over current and to reduce the DC-link overvoltage for improving the operational safety of WT [9]. But this scheme is not able to reduce the oscillation of electromagnetic torque which might be harmful to the gearbox in some extreme situations [10]. The two economical solutions for large-scale wind farm, Static Synchronous Compensators (STATCOM) connected in parallel with the transmission line of the wind farm can inject a large amount of reactive power for boosting the terminal voltage of the wind farm during grid fault [11], and Dynamic Voltage Restorers (DVRs) connected in series with the transmission line can compensate the missing terminal voltage directly through a grid-connected transformer [12]. Besides, another solution cheaper than DVR is the use of fault current limiter (FCL) like series dynamic braking resistor [13] and bridge-type fault current limiter [14]. By using a power switch circuit to execute the conversion between normal and fault operation, the FCL can enlarge the equivalent impedance of transmission line to reduce the over-currents in both the stator and rotor-side during grid faults.

In order to solve the problems of FRT capacity and unsteady output power simultaneously, the modified controls of the RSC and superconducting coil (SC) in a superconducting magnetic energy storage-fault current

equivalent high inductance induced in the stator could limit fault current effectively.

(ii) The SC also acts as an energy storage device to absorb the surplus energy in the DC-link capacitor. With the control of the DC-DC converter, the DC-link over-voltage hence could be reduced.

Table 1 Parameters for the DFIG and SMES-FCL.

| | Parameter | Value |
|----------|--|----------------------|
| DFIG | rated power of DFIG | 1.5 MW |
| | stator voltage/frequency | 690 V/50 Hz |
| | rotor voltage/frequency | 1533 V/12 Hz |
| | DC-link voltage | 1200 V |
| | stator/rotor resistance | 0.0049 pu, 0.0055 pu |
| | stator/rotor leakage inductance | 0.1386 pu, 0.1493 pu |
| | magnetising inductance | 3.9 pu |
| SMES-FCL | rated power of isolation transformer | 50 kVA |
| | stator side and rectifier side voltage of isolation transformer | 230 V/690 V |
| | stator side/rectifier side resistance of isolation transformer | 0.005 pu, 0.005 pu |
| | stator side/rectifier side leakage inductance of isolation transformer | 0.035 pu, 0.035 pu |
| | magnetising inductance of isolation transformer | 500 pu |
| | SC inductance | 70 mH |

Table 2 Switching operations of the DC-DC converter

| Mode (g1, g2) | Normal operation | During faults |
|------------------------|------------------|---------------------------------------|
| (OFF, OFF) | discharging SC | discharging SC |
| (ON, ON) | charging SC | charging SC limiting fault current |
| (ON, OFF) or (OFF, ON) | locking | locking |

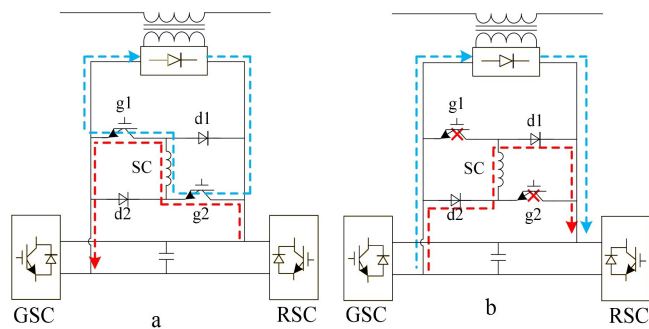


Fig 2 Current flow diagrams in SMES-FCL under different switching operation (a) g1 and g2 turned ON (b) g1 and g2 turned OFF

IV. Rotor-side mathematical model and parameter estimation of SC

The proposed system is aimed at constraining the instantaneous rotor current below 2.0 pu to protect RSC controller. Owing to the coupling correlation existed between the rotor and stator currents, the latter will be constrained simultaneously. From the equivalent rotor circuit in Fig. 3a, the rotor dynamic equation can be expressed by

$$v_r - v_{r0} = R_r i_r + L_r' \frac{d}{dt} i_r \quad (6)$$

where v_r is the rotor output voltage, and v_{r0} the rotor winding voltage induced by stator flux. R_r' and L_r' are equivalent transient rotor resistance and inductance, respectively, and can be expressed by [19]

$$R_r' = R_r + (L_m/L_m + L_l's)^2 R_s \quad (7)$$

$$L_r' = L_m + L_{lr} - (L_m^2/L_m + L_l's) \quad (8)$$

where L_{lr} is the rotor leakage inductance and L_m the mutual inductance. R_s and R_r are stator and rotor resistance, respectively. $L_l's$ is the equivalent stator inductance, which can be expressed by

$$L_l's = L_{ls} + L_{lt} + nL_{sc} \quad (9)$$

Where L_{ls} is the stator leakage inductance, L_{lt} the isolation transformer leakage inductance, L_{sc} the SC inductance, and n the ratio of the transformer. Assume that a symmetrical fault occurs in the grid at time $t = 0$, and the terminal voltage V_s drops to $V_s(1-p)$, where p is the voltage dip ratio. Consider that the peak value will reach at the time of $T/2$ (T is the grid period), the rotor peak current value can be expressed by equation (10) where ω_s and ω_r are stator and rotor electrical angular frequency, respectively. V_{rm} is the maximum output voltage of RSC, $ks = L_m/L_s$ the stator coupling factor, s the DFIG slip, and $i_r(0^-)$ is the pre-fault rotor current value.

From equation (10), with the increase in the L_{sc} value, the I_{rp} will decrease accordingly. However, a larger L_{sc} will lead to a higher time constant τ_s that causes a slower recovery speed of DFIG output power (P_{DFIG}), electromagnetic torque (T_{em}), and other relevant parameters after the fault. Hence, the optimised value of L_{sc} should be the minimum inductance to limit the peak rotor current value under 2.0 pu. Consider that $p = 1$ and $I_{rp} = 2.0$ in Fig. 3b, the optimised value of L_{sc} approximately 163 mH.

$$\begin{aligned} \left| \vec{i}_{rp} \right| = I_{rp} = & \left| \frac{V_{rm} - k_s s V_s (1-p)}{R_r' + j s \omega_s L_r'} e^{j s \omega_s \frac{T}{2}} + \frac{k_s V_s p (1-s)}{R_r' - j \omega_r L_r'} e^{-(j \omega_s + R_r'/L_r') \frac{T}{2}} \right. \\ & \left. + \left(\vec{i}_r(0_-) - \frac{V_{rm} - k_s s V_s (1-p)}{R_r' + j s \omega_s L_r'} - \frac{k_s V_s p (1-s)}{R_r' - j \omega_r L_r'} \right) e^{\frac{T R_r'}{2 L_r'}} \right| \quad (10) \end{aligned}$$

V. Control strategy

A. Control strategy of SMES-FCL

Fig. 3 shows the control strategy of SMES-FCL. It can be divided into two parts. During normal operation, the input signal from the difference between the actual output power P_{DFIG} of DFIG and the reference output power P_{DFIG_ref} plays a main role in smoothing output power. By PI-1 controller, the input signal is transformed to the change of DC-link voltage signal, which is used to regulate the reference DC-link voltage. By controlling the reference DC-link voltage, the GSC output power can be automatically adjusted to smooth the DFIG total output power. PI-2 controller is used to transform the difference between actual and reference DC-link voltage to a duty cycle deviation (ΔD) signal. By adding 0.5 and ΔD , the duty cycle (D) can be utilised to control the PWM signals. When D is higher than 0.5, SC will be charged and the DFIG total output power will decrease. Otherwise, when D is lower than 0.5, SC will be discharged and the DFIG total output power will increase.

During a fault, the control strategy of SMES-FCL is aimed at maintaining the DC-link voltage to constant. Since the DC-link voltage will increase during the fault, the SC will absorb electrical energy from the DC-link capacitor. Consider that DFIG total output power P_{DFIG} has a positive correlation with the terminal voltage, the P_{DFIG} is thus multiplied by the average value of terminal root-mean-square (RMS) voltage V_{g_avg} in Fig. 3. Hence, $V_{g_rms_avg}$ is nearly zero for preventing P_{DFIG} to disturb the control of VDC under a symmetrical fault (3LG).

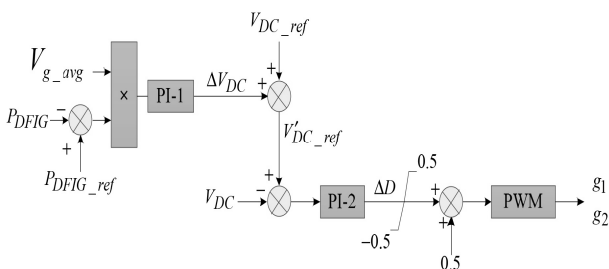


Fig 3 Control scheme of SMES-FCL

B. Control strategies of GSC and RSC

Fig. 4 shows the control scheme of GSC. Using the input signals of ΔV_{DC} and difference of grid reactive power

(ΔQ_g), the GSC controller is mainly utilised to maintain DC-link voltage to constant and to control the energy exchange between the rotor side and stator side. The equation for DC-link voltage control can be expressed by [20]

$$I_{gd}^* = (V_{DC}^* - V_{DC}) (kp + ki/s) \quad (11)$$

where kp and ki are the PI parameters, and V^*DC is the reference value of VDC.

The $d-q$ current references i_{gd}^* and i_{gq}^* are generated by PI-1 and PI-2 controllers with the input signals. The generated i_{gd}^* and i_{gq}^* are compared with the actual $d-q$ currents i_{gd} and i_{gq} and the resulting difference values are served as the input signals of PI-3 and PI-4 controllers. The PI-3 and PI-4 controllers generate the $d-q$ voltage signals v'_{gd} and v'_{gq} . The two voltage signals are compensated by $v_{sd} + \omega_s L_g i_{gq}^*$ and $-\omega_s L_g i_{gd}^*$, and then import into PWM model to generate the IGBT control signals. R_c and L_c are the stator-to-grid coupling resistance and inductance. Fig. 5 gives the overall control scheme in the RSC controller. It should be noted that the RSC controller is aimed at achieving the decoupling control of active and reactive power via stator flux oriented vector control by using the difference of angular frequency ($\Delta \omega_r$) and stator side reactive power (ΔQ_s) as its input signals.

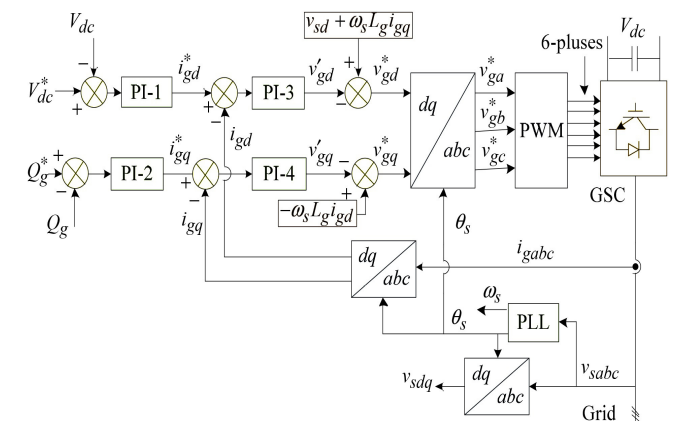


Fig.4 GSC Control scheme

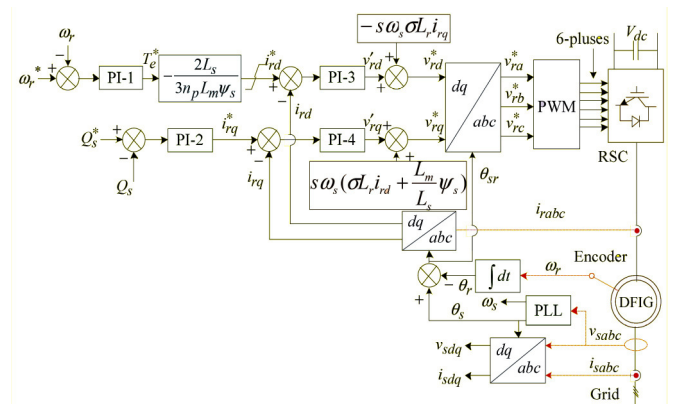


Fig.5 RSC Control scheme

C. Positive-sequence d-q current modification control of RSC

Although SMES-FCL has a good performance to restrain fault over current and to smooth output power, the addition of the SC will increase the time constant τ_s , which slows the recovery time of the whole system and leads to a certain fluctuation of T_{em} after a fault. Besides, the varying wind speed during normal operation can also lead to a certain fluctuation of T_{em} . The dynamic equation about T_{em} can be expressed by [21]

$$T_{em} = (3/2)np(Lm/Ls)((\psi_{sq}i_{rd} - \psi_{sd}i_{rq})) \quad (12)$$

Since the effects of i_{rd} and i_{rq} are decoupled, means that d -axis rotor current signals i_{rd} can be used to maintain T_{em} . In the proposed control method, the reference i_{rd} is mainly used to maintain T_{em} . The reference i_{rq} is always used to maintain reactive power. Since the smoothed reactive power could help to smooth the T_{em} , we also use i_{rq} as a control signal. Note that the fluctuation of T_{em} after a fault or during varying wind speed is always caused by positive sequence of stator/rotor current, so the control scheme in Fig. 6 uses i_{rd1} and i_{rq1} as input signals. The reference signals i_{rd1_ref} and i_{rq1_ref} are the function of the stator voltage V_s , as can be seen in Fig. 7. K_d is the gain of the control signals, it is related to DFIG resistance, inductance, and so on.

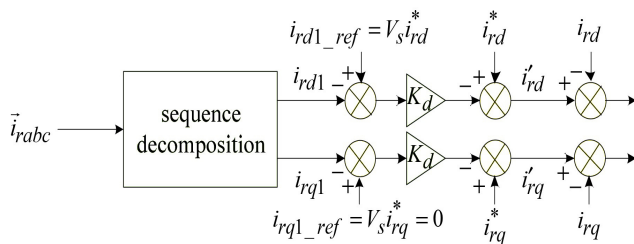


Fig.6 Positive-sequence d-q current modification control scheme

VI. SIMULATION RESULTS AND ANALYSES

Simulation is done using MATLAB/SIMULINK software. The 1.5MW wind turbine model connected with grid is built in simulink using the parameters given in table 1. To prove the effectiveness of the SMES-FCL in smoothing the DFIG output power and enhancing the FRT capability, simulation is done by considering different fault conditions: ii) three-phase-to-ground (3LG) fault, two-phase-to ground (2LG) fault and a single-phase-to-ground (1LG) fault occur at 0.3 s, 0.5 s and 0.7 s, respectively with fault resistances of 1 mΩ.

Figure 7 shows simulink model for grid connected DFIG model. In this model the stator is connected directly to the grid and rotor is connected via two back to back converter called RSC and GSC. A DC link capacitor is connected between these two converters. The main purpose of having these RSC and GSC is to control the DFIG. The 1.5MW DFIG generates stator voltage of 690V which is connected to the grid through 33KV/690V transformer. The DC link voltage is maintained at 1200V.

Figure 8 shows the rotor current of DFIG during normal condition. The fault conditions of three-phase-to-ground (3LG) fault, two-phase-to ground (2LG) fault and a single-phase-to-ground (1LG) fault is simulated at 0.3s, 0.5s and 0.7s, respectively. Figure 9 shows the occurrence of fault in rotor current which shows the peak value of fault current reaches up to 4.0p.u. Our main objective is to reduce the peak current value to below 2.0p.u.

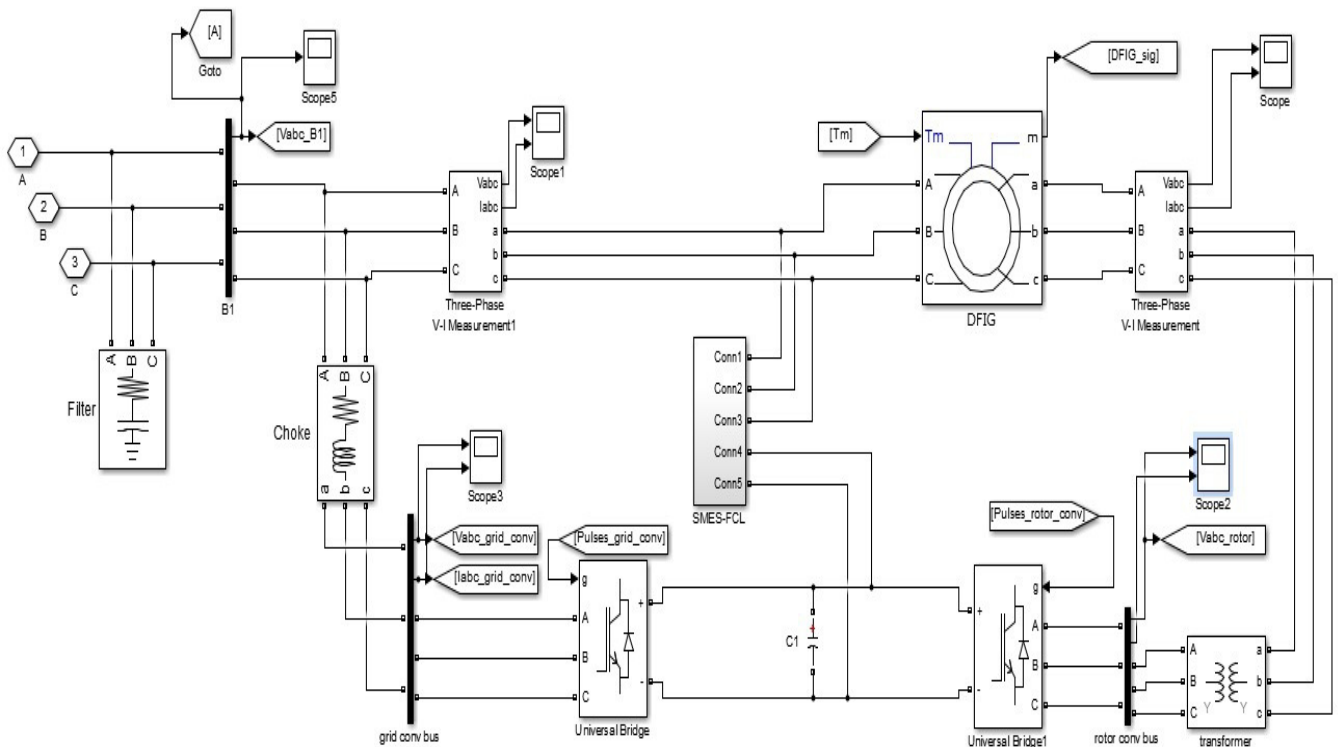


Fig. 7 Simulink model for grid connected DFIG model.

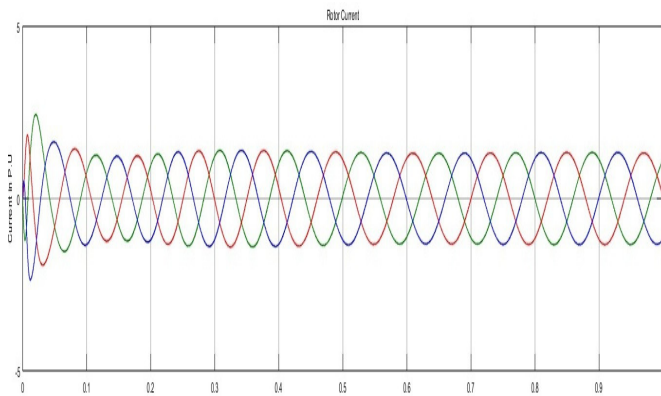


Fig. 8 Rotor current of DFIG during normal condition.

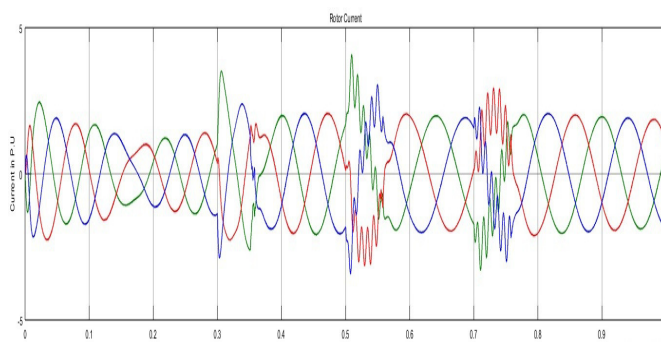


Fig. 9 Rotor current of DFIG during fault conditions

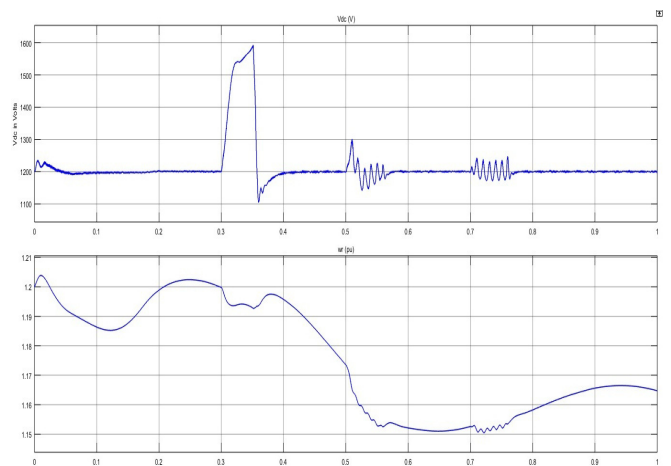


Fig.10 DC link voltage and rotor speed during fault conditions

Figure 10 shows the DC link voltage during fault conditions and it shows the voltage rises to 1800V, which has to be controlled and maintained within tolerable limit.

Figure 11 shows the simulink model for SMES-FCL connected with DFIG model. It consists of two quadrant chopper connected with Superconducting Coil (SC) which is controlled using PWM signal. These PWM signal is generated by using the control circuit given in the figure 4.

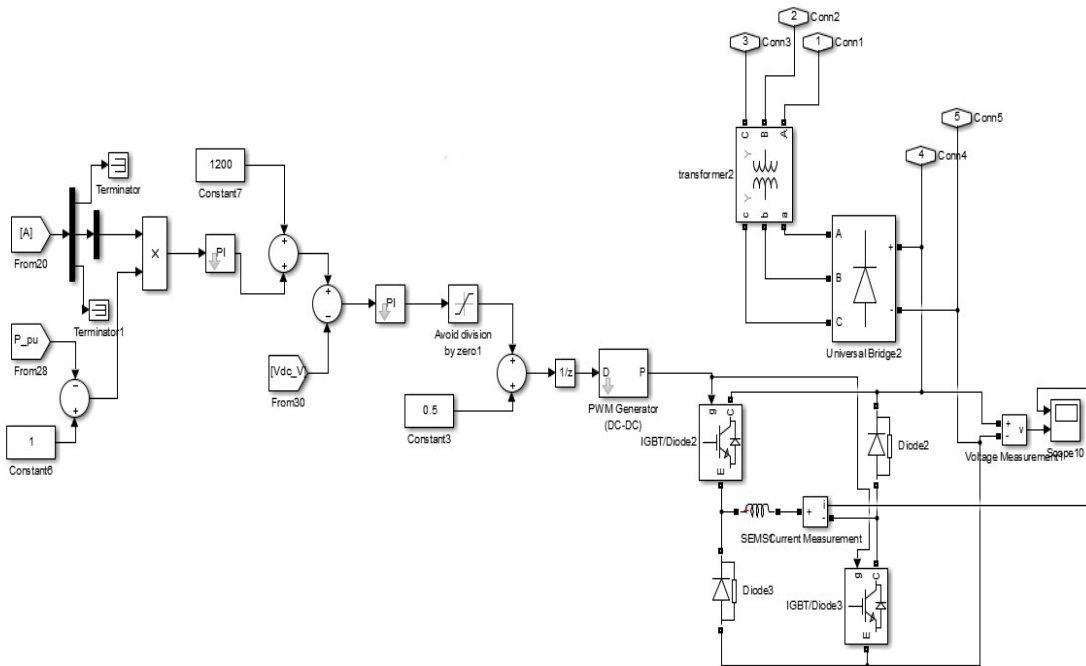


Fig.11 Simulink model for SMES-FCL connected with DFIG model.

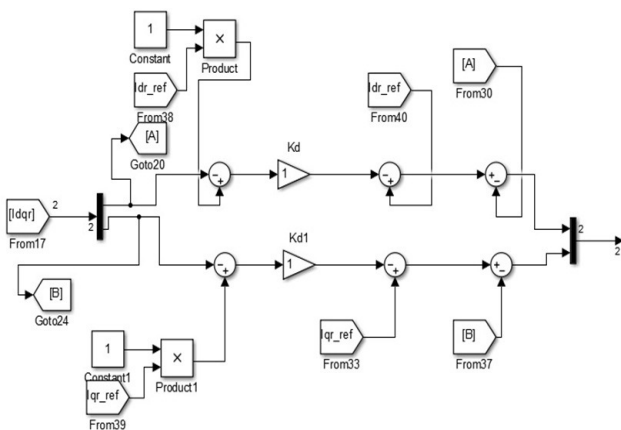


Fig. 12 Simulink model for positive-sequence d-q current modification

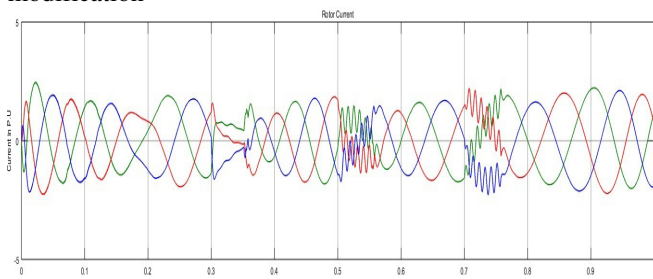


Fig. 13 Rotor current of DFIG during fault conditions with SMES-FCL

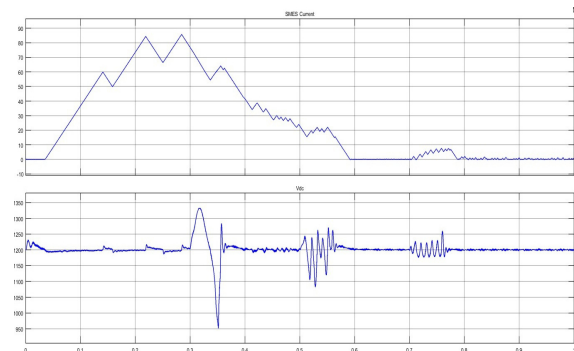


Fig. 14 DC link voltage during fault conditions with SMES-FCL

Based on the output power and DC link voltage ,the PWM signal is generated and from the control circuit it is observed that, if the value of duty cycle is greater than 0.5 ,it indicates that there is surplus power which have to be absorbed by SC by turning ON g1,g2 i.e., SC is in charging state. In the similar way during fault conditions, the rise in DC link voltage gets absorbed by SC, which results in reduced peak value of fault current. Likewise, if the output power is below the allowable limit, the stored energy in the SC gets discharged by turning OFF g1, g2 in order to maintain the smoothed output power.

Figure 13 shows the rotor current after the application of SMES-FCL. From the figure it is observed that the peak value of rotor current get reduced to below 2.0p.u, as a result our converters get protected. Figure14 shows the DC link voltage during fault conditions with SMES-FCL and it shows that the value of Vdc get reduced to tolerable value.

Further the positive sequence current modification is done in the rotor control circuit which is shown in figure 12. As the d -axis rotor current signals i_{rd} is used to maintain T_{em} the proposed control method, utilize the reference i_{rd} in maintaining T_{em} . The reference i_{rq} is always used to maintain reactive power. Since the smoothed reactive power could help to smooth the T_{em} , we also use i_{rq} as a control signal. It is observed that the fluctuation of T_{em} after a fault or during varying wind speed is always caused by positive sequence of stator/rotor current, so the control scheme uses i_{rd1} and i_{rq1} as input signals. From the output it is observed that the recovery time after the occurrence of fault gets shorten due to positive sequence current modification which further improves the transient stability of DFIG system.

VII. CONCLUSION

The SMES-FCL based protection scheme by modified control of GSC and RSC has been proposed for enhancing the FRT capability and to improve the transient power stability of the DFIG. The modelling of the SMES-FCL based DFIG and the parameter estimation of SC have been discussed. Simulation results obtained from a 1.5 MW DFIG-based WT shows the feasibility and effectiveness of the SMES-FCL based protection scheme under various symmetrical and asymmetrical faults. With an additional PCM control, this scheme has also been verified to lower the requirement of SC current capacity, to shorten the recovery time duration after grid faults, and to smooth the output power of the DFIG during normal operations. Therefore, the SMES-FCL based protection method could be able to provide an integrated protection to the whole DFIG during normal and faults conditions.

REFERENCES

- [1] Yang, L., Yang, G.Y., Xu, Z., *et al.*: 'Optimal controller design of a doublyfed induction generator wind turbine system for small signal stability enhancement', *IET Gener. Transm. Distrib.*, 2010, **4**, (5), pp. 579–597
- [2] Cartwright, P., Holdsworth, L., Ekanayake, J.B., *et al.*: 'Co-ordinated voltage control strategy for a doubly-fed induction generator (DFIG)-based wind farm', *IEE Proc.-Gener. Transm. Distrib.*, 2004, **151**, (4), pp. 495–502
- [3] Rashid, G., Ali, M.H.: 'Transient stability enhancement of doubly fed induction machine-based wind generator by bridge-type fault current limiter', *IEEE Trans. Energy Convers.*, 2015, **30**, (3), pp. 939–947
- [4] Muller, S., Deicke, M., De Doncker, R.W.: 'Doubly fed induction generator systems for wind turbines', *IEEE Ind. Appl. Mag.*, 2002, **8**, (3), pp. 26–33
- [5] D. Zhu, X. Zou, L. Deng, Q. Huang, S. Zhou, Y. Kang, "Inductanceemulating control for DFIG-based wind turbine to ride-through grid faults," *IEEE Trans. Power Electron.*, vol.32, no.11, pp.8514-8525,2017.
- [6] Xiang, D.W., Ran, L., Tavner, P.J., *et al.*: 'Control of a doubly fed induction generator in a wind turbine during grid fault ride-through', *IEEE Trans.Energy Convers.*, 2006, **21**, (3), pp. 652–662
- [7] Lopez, J., Sanchis, P., Gubia, E., *et al.*: 'Control of doubly fed induction generator under symmetrical voltage dips'. 2008 IEEE Int. Symp. On Industrial Electronics, Cambridge, UK, 2008, pp. 2456–2462
- [8] Zou, Z.C., Chen, X.Y., Li, C.S., *et al.*: 'Conceptual design and evaluation of a resistive-type SFCL for efficient fault ride through in a DFIG', *IEEE Trans.Appl. Supercond.*, 2016, **26**, (1), p. 5600209
- [9] Abad, G., López, J., Rodríguez, M., *et al.*: 'Doubly Fed induction machine: modeling and control for wind energy generation' (Wiley-IEEE Press, Hoboken, NJ, USA, 2011)
- [10] Gounder, Y.K., Nanjundappan, D., Boominathan, V.: 'Enhancement of transient stability of distribution system with SCIG and DFIG based wind farms using STATCOM', *IET Renew. Power Gener.*, 2016, **10**, (8), pp. 1171–1180
- [11] Hossain, M.M., Ali, M.H.: 'Transient stability improvement of doubly fed induction generator based variable speed wind generator using DC resistive fault current limiter', *IET Renew. Power Gener.*, 2016, **10**, (2), pp. 150–157
- [12] Ramirez, D., Martinez, S., Platero, C.A., *et al.*: 'Low-voltage ride-through capability for wind generators based on dynamic voltage restorers', *IEEE Trans. Energy Convers.*, 2011, **26**, (1), pp. 195–203
- [13] Okedu, K.E.: 'Enhancing DFIG wind turbine during three-phase fault using parallel interleaved converters and dynamic resistor', *IET Renew. Power Gener.*, 2016, **10**, (8), pp. 1211–1219
- [14] Rashid, G., Ali, M.H.: 'Nonlinear control-based modified BFCL for LVRT capacity enhancement of DFIG based wind farm', *IEEE Trans. Energy Convers.*, 2017, **32**, (1), pp. 284–295
- [15] X. Y. Xiao, R. H. Yang, X. Y. Chen, Z. X. Zheng, C. S. Li. "Enhancing FRT capability of DFIG with modified SMES-FCL and RSC control," *IET Gener. Transmiss. Distrib.*, vol. PP, no. 99, pp. 1-10, 2017. (doi: 10.1049/iet-gtd.2016.2136)
- [16] Okedu, K.E., Muyeen, S.M., Takahashi, R., *et al.*: 'Wind farms fault ride through using DFIG with new protection scheme', *IEEE Trans. Sustain. Energy*, 2012, **3**, (2), pp. 242–254
- [17] Varol, A., Ilkilic, C., Varol, Y.: 'Increasing the efficiency of wind turbines', *J.Wind Eng. Ind. Aerodyn.*, 2001, **89**, (9), pp. 809–815
- [18] Sun, T., Chen, Z., Blaabjerg, F.: 'Transient stability of DFIG wind turbines at an external short-circuit fault', *Wind Energy*, 2005, **8**, (3), pp. 345–360
- [19] Guo, W.Y., Xiao, L.Y., Dai, S.T.: 'Enhancing low-voltage ride-through capability and smoothing output power of DFIG with a superconducting fault current limiter–magnetic energy storage system', *IEEE Trans. Energy Convers.*, 2012, **27**, (2), pp. 277–295
- [20] Zou, Y., Elbuluk, M.E., Sozer, Y.: 'Simulation comparisons and implementation of induction generator wind power systems', *IEEE Trans.Ind. Appl.*, 2013, **49**, (3), pp. 1119–1128
- [21] Ou, R., Xiao, X.Y., Zou, Z.C., *et al.*: 'Cooperative control of SFCL and reactive power for improving the transient voltage stability of grid-Connected wind farm with DFIGs', *IEEE Trans. Appl. Supercond.*, 2016, **26**, (7), p.5402606